Coherent Spontaneous Hemodynamics in the Human Brain

Cristianne Fernandez, Tapan Das, Giles Blaney, Zachary Haga, Thomas McWilliams, Julia Mertens, Angelo Sassaroli, and Sergio Fantini

***Abstract*—*Goal:* This work investigates the presence of cerebral hemodynamics (namely Oxy (O) and Deoxy (D) hemoglobin concentrations) that are coherent with spontaneous oscillations in Arterial Blood Pressure (ABP) in 78 healthy subjects during a driving simulation task. *Methods:* Spatially resolved O and D were measured on the prefrontal cortex with multi-channel near-infrared spectroscopy (NIRS). Wavelet coherence and phasor analysis were performed between O and ABP, and between D and ABP to evaluate the amplitude ratio, phase difference, and duration of significant coherence. *Results*: In the low-frequency range, oscillations at 0.1 Hz featured significant coherence for the longest time fraction (∼10%–30%). At this frequency, the amplitude ratio and phase difference showed a greater variance across subjects than over cortical locations, and no significant difference between driving tasks and baseline. *Conclusions*: Measuring low-frequency cerebral hemodynamics that are coherent with systemic ABP holds promise for non-invasive assessment of cerebral perfusion and autoregulation at the cerebral microvascular level.**

***Index Terms*—Near infrared spectroscopy, spontaneous oscillations, transfer function analysis, coherent hemodynamics.**

***Impact Statement*—Spontaneous cerebral hemodynamics measured with near-infrared spectroscopy feature a significant coherence with systemic arterial blood pressure for about 10%–30% of the time at a relevant autoregulation frequency of 0.1 Hz.**

I. Introduction

NEAR-Infrared Spectroscopy (NIRS) is a non-invasive optical technique that can measure concentration changes in Oxy(ΔO) and Deoxy hemoglobin (ΔD) in the outermost layers of the cerebral cortex [1]. Cerebral hemodynamics measured with NIRS result from a combination of cardiac pulsation (∼1 Hz), respiration (∼0.2–0.5 Hz) [2], low-frequency oscillations (LFOs) (Mayer waves; ∼0.1 Hz) [3], and very low-frequency oscillations (∼0.01–0.05 Hz) [2] that are mostly driven by Arterial Blood Pressure (ABP) fluctuations. Spontaneous LFOs of systemic and cerebral vessels are affected by neuronal [4], metabolic [5], myogenic stimuli [6] and sympathetic changes [7]. LFO's have been investigated using NIRS, Transcranial Doppler ultrasound (TCD), and other techniques for fundamental, functional connectivity and autoregulation studies [8].

Transfer Function Analysis (TFA) has been used in TCD to investigate the frequency dependence of gain and phase for coherent oscillations of Cerebral Blood Flow Velocity (CBFV) and ABP [9], but this technique is limited in that it cannot measure micro-vasculature and localized changes in cerebral blood flow. A number of systematic studies on detection of LFOs by NIRS on human subjects have been reported [6], [10], [11], mainly focusing on 0.1 Hz. Over a range of frequencies, the highest coherence between cerebral hemodynamics and ABP lies around 0.1 Hz [6], [12] but have been limited in the number of subjects investigated. Spontaneous oscillations have lower coherence than induced oscillations [13], but are relevant when inducing oscillations is not feasible. The motivation behind this work is to look at the amplitude ratio, phase shift and coherence in hemodynamic parameters of spontaneous oscillations in a relatively large data set.

Here we report a study on 78 healthy human subjects involved in a simple driving task with a series of braking events with the goal to evaluate the use of spontaneous coherent hemodynamics. The time of coherent oscillations during 3-minute periods were evaluated over a large range of subjects to assess the extent to which spontaneous oscillations feature significant coherence. Transfer function analysis was done to evaluate the relative amplitude and phase between cerebral hemodynamics and ABP, at 0.1 Hz, to evaluate variance within and across subjects. Lastly, the baseline driving condition and periods with braking events were compared to evaluate the impact of brain activation on coherent spontaneous cerebral hemodynamics.

II. Materials and Methods

A. Study Protocol and Data Acquisition

A total of 78 subjects (42M, 36F, 18–39 years old) participated in 2 sessions in a Tufts University Institutional Review

Manuscript received 21 October 2022; revised 19 December 2022 and 30 December 2022; accepted 30 December 2022. Date of publication 3 January 2023; date of current version 22 May 2023. This work was supported by the Air Force Office of Scientific Research (AFOSR) under Grant FA9550-18-1-0465 and in part by the National Institutes of Health (NIH) under Grants R01-NS095334 and R01-EB029414. *(Corresponding author: Cristianne Fernandez.)*

Cristianne Fernandez, Tapan Das, Giles Blaney, Angelo Sassaroli, and Sergio Fantini are with the Department of Biomedical Engineering, Tufts University, Medford, MA 02155 USA (e-mail: cristianne.fernandez@tufts.edu; tapan.das@tufts.edu; giles.blaney@tufts.edu; angelo.sassaroli@tufts.edu; sergio.fantini@tufts.edu).

Zachary Haga is with the Department of Computer Science, Tufts University, Medford, MA 02155 USA (e-mail: zachary.haga@tufts.edu).

Thomas McWilliams and Julia Mertens are with the Department of Psychology, Tufts University, Medford, MA 02155 USA (e-mail: thomas.mcwilliams@tufts.edu; julia.mertens@tufts.edu).

Digital Object Identifier 10.1109/OJEMB.2023.3234012

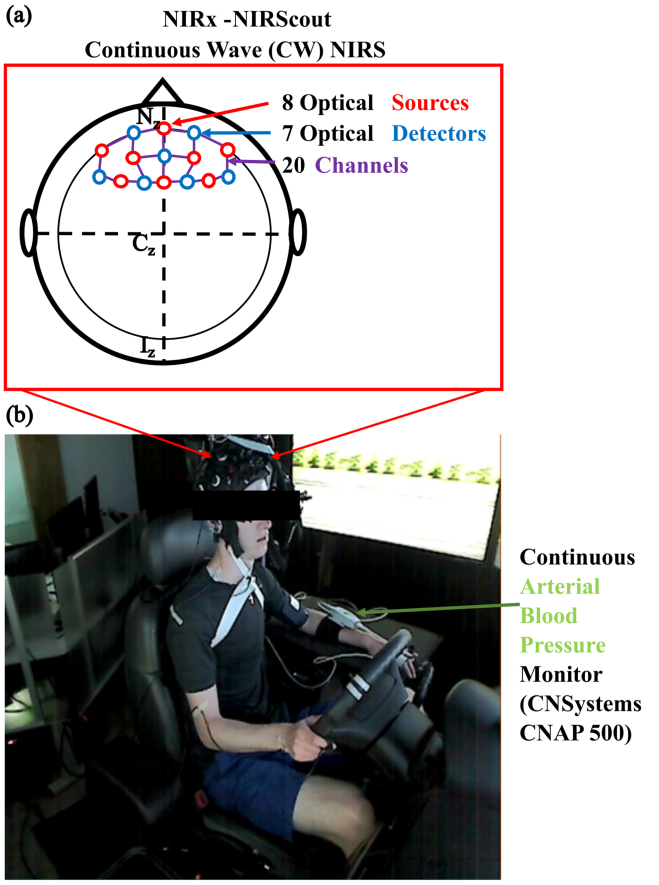

Fig. 1. (a) Schematic of the location of the 8 optical sources and 7 detectors from the continuous-wave near-infraRed spectroscopy (CW-NIRS) instrument on the human head. (b) Experimental set-up where a subject is seated with the CW-NIRS device on their head and the beat-to-beat finger plethysmography system for arterial blood pressure (ABP) measurements on their fingers and upper arm.

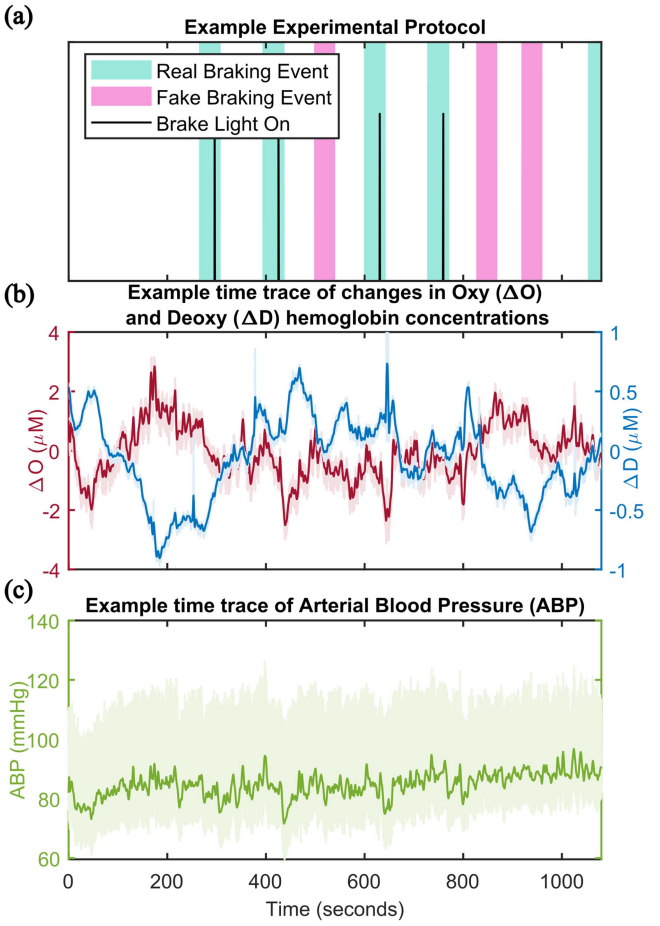

Fig. 2. (a) Example protocol with the time markings of real and fake braking events and for when the leading cars brake lights turned on. (b) Time trace of the changes in oxy (ΔO) and deoxy (ΔD) hemoglobin concentrations from one channel. (c) Time trace of the arterial blood pressure (ABP) for the same subject. For (b) and (c) the solid lines depict the signal low-passed to 0.2 Hz and shaded region encompasses unfiltered data.

Board (IRB) approved study (protocol number: 1802002, approval date: 02/14/2018). Continuous Wave (CW) NIRS and ABP measurements were performed while the subject was in a medium fidelity partial-cab driving simulator (RTI, Ann Arbor, MI), which has been previously described [14]. CW-NIRS measurements were acquired with a NIRScout system (NIRx Medical Technology, Berlin, Germany) sampled at 7.81 Hz. The instrumental configuration consisted of 8 light-emitting diode (LED) sources (wavelengths: 760 and 850 nm) and 7 Photo-Diode (PD) detectors, which resulted in 20 Single-Distance (SD) measurement channels at a source-detector spacing of 30 mm on the pre-frontal cortex (Fig. 1(a)). A beat-to-beat finger plethysmography system (NIBP100D, BIOPAC Systems, Goleta, CA) used to measure non-invasive ABP [15] using changes in blood volume in the artery was placed on the subjects' left fingers and upper arm, and data were sampled at 20 Hz. Fig. 1(b) depicts the driving simulator set up with the ABP and CW-NIRS instruments connected to the subject.

The experimental protocol consisted of a baseline period with uneventful, constant-speed driving for approximately 3 minutes on a 2-lane highway. Participants than engaged in a total of 10 events, which were ordered randomly for each subject and session. Six events were labeled as real braking (where the participant needed to brake to avoid a collision with a leading car that was braking in front of them) and four fake braking (where the leading car appeared but did not brake). An example experimental protocol can be seen in Fig. 2(a), where the black line indicates where the leadings cars brake lights turned on and the shaded region when the car was in front of the participants car.

B. Near-InfraRed Spectroscopy and Arterial Blood Pressure Data Processing

Methods described here were applied to each subject, experiment, and SD channel independently. NIRS intensity measurements for both wavelengths and the ABP signal were synchronized and interpolated to 20 Hz. NIRS measurements were evaluated for artifacts due to non-physiological changes by linear piecewise detrending which identified sections in which the variance of the signal is above the 75th and below the 25th percentiles and used these as breakpoints in the detrend. The ΔO

and ΔD were calculated using the modified Beer Lambert Law [16] with a wavelength dependent Differential Pathlength Factor (DPF) [16], [17]. NIRS channels recording non-physiological variation over 1 μM were disregarded [18], as data with this high non-physiological noise would mask those of systematic oscillations. Example time traces of ΔO and ΔD can be seen in Fig. 2(b) and of ABP in Fig. 2(c), where the solid line shows the signal low-passed to 0.2 Hz for visualization and the shaded region is the original signal that reflects systolic-diastolic variations.

C. Transfer Function and Coherence Analysis

Transfer function and coherence analysis between the hemodynamic signals (ΔO and ΔD) and ABP were performed using previously described methods [16], [19], [20]. Data were then sectioned into a total of six 3-minute non over lapping blocks, where the first 3-minute block (minutes 0 to 3) is referred to as the baseline. Each block was than processed independently.

Time-frequency maps of the wavelet coherence between ΔO and ABP, and ΔD and ABP were calculated using a modified version of MATLAB's wcoherence function that removes smoothing in frequency. A coherence threshold generated using random surrogate data (alpha level = 0.05) [21], [22] was applied so that only pixels in time and frequency that have a statistically significant coherence were evaluated. Multiple comparisons were not accounted for. A logical AND was taken between the ΔD-ABP and ΔO-ABP maps to create a significant coherence map used for ΔD and ΔO. TFA between time signals of ΔO and ABP, ΔD and ABP, and ΔD and ΔO for each block was performed using the continuous wavelet transform with a complex Morlet mother wavelet to find the phasor ratio maps of **O/ABP**, **D/ABP**, and **D/O** in time and frequency [16], [19], [20]. This resulted in the amplitude ratio and the phase difference between the two parameters across time and frequency.

D. Coherence Requirements and Spontaneous Oscillation Frequencies

Coherent spontaneous oscillations within the range of 0.01–1.5 Hz were considered. A series of central frequencies and their bandwidths (as determined by the half power bandwidth of a sinusoidal wave at that central frequency [19]) were found. Maps of significant coherence for **O** and **ABP**, **D** and **ABP**, and the logical AND were further filtered to require that in each frequency band of interest, significant coherence lasted longer than one period of the central frequency and significant coherence at the central frequency. Filtered maps were applied to the phasor ratio maps so that only pixels in time and frequency with statistically significant coherence that passed the requirements were considered in further analysis. The logical map between ΔD-ABP and ΔO-ABP was applied to the phasor ratio map of **D/O**. An average phasor ratio was computed for **O/ABP**, **D/ABP**, and **D/O** over each frequency band, resulting in one value for each block (6), channel (20), subject (78), and session (2) across frequencies.

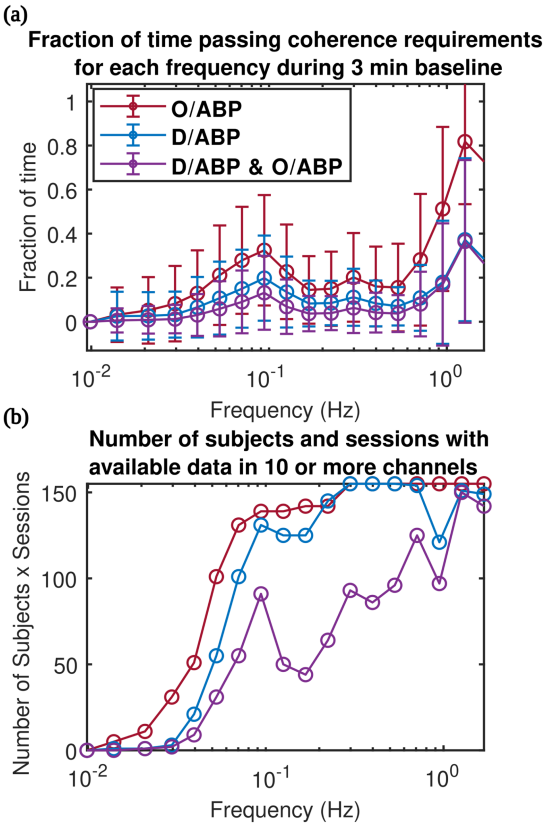

Fig. 3. (a) Fraction of time during baseline in which the coherence requirements where met for each frequency for oxy (**O**) hemoglobin versus arterial blood pressure (**ABP**) (**O/ABP**), deoxy (**D**) hemoglobin versus ABP (**D/ABP**) and the logical AND the two across all channels, subjects and sessions. (b) Number of subjects across frequency in which there where 10 or more channels that passed the coherence requirements.

III. Results

A. Availability of Coherent Hemodynamics

The fraction of time, during baseline, for which the coherence requirements were fulfilled (statistically significant coherence for at least 1 period of the central frequency) across frequency are shown in Fig. 3(a) for **O/ABP**, **D/ABP** and for the logical AND between **O/ABP** and **D/ABP**. The values for each channel, subject, and experiment were treated as independent data points. Fig. 3(b) depicts the number of subjects that had significant data in 10 or more NIRS channels. The highest fraction of time with coherence occurred at ∼1 Hz, which is indicative of the heart rate. At this frequency, **O/ABP** has the highest fraction of coherence as arterial pulsation results in hemodynamic oscillations that are mostly associated with oxyhemoglobin (oxygen saturation of arterial blood is close to 100%). Large arterial oscillations can be seen in Fig. 2(b), while ΔD has a smaller contribution.

In the range of physiologically relevant frequencies for assessing cerebral health (∼0.01–0.1 Hz) [8], [23], the highest fraction of time of coherence occurred at ∼0.1 Hz with on average ∼32% for **O/ABP**, ∼19% for **D/ABP**, and ∼13% for **D/O**. Out of 158 data sets there were 139, 131, and 91 available

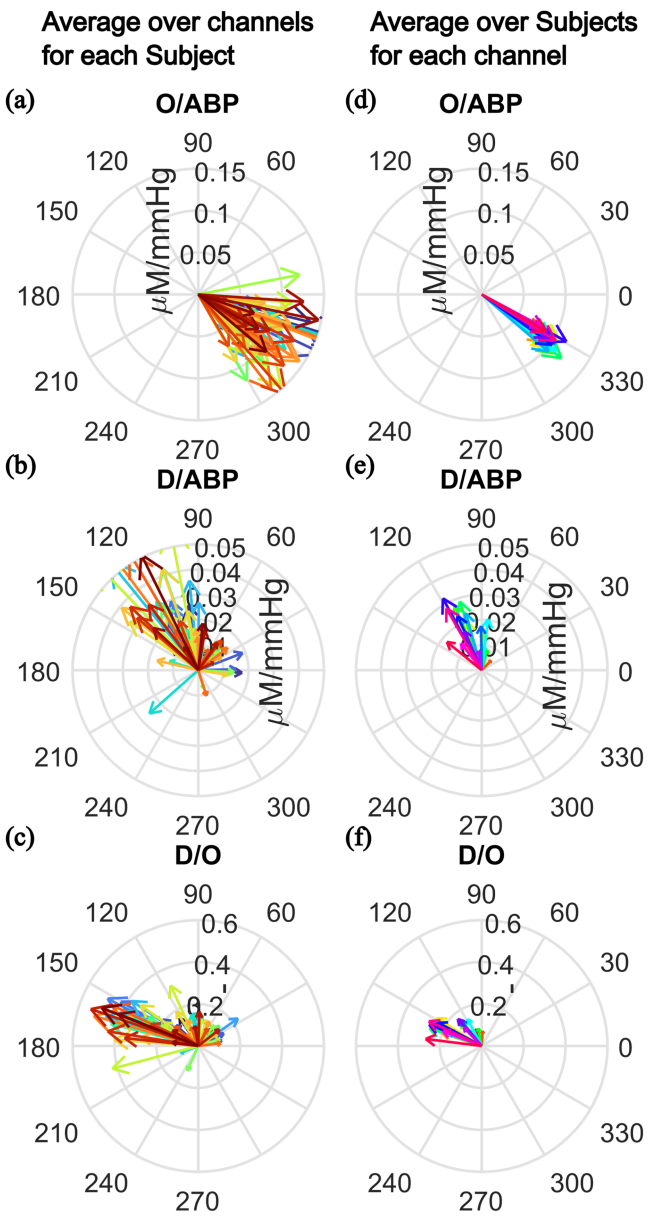

Fig. 4. Average phasor ratios over channels for each subject (a, b, and c) at 0.1 Hz and the average phasor ratios over subjects for each channel (d, e, and f). (a) and (d) show the phasor ratios between oxy (**O**) hemoglobin and arterial blood pressure (**ABP**), (b) and (e) show the phasor ratio between deoxy (**D**) hemoglobin and **ABP**, and (c) and (f) show the phasor ratio between **D** and **O**.

for the respective data types. At all frequencies, **O/ABP** showed the largest fraction followed by **D/ABP**. The logical condition is the lowest on average which shows that **D** is not always coherent with **ABP** when **O** is coherent with **ABP**. This indicates that both hemodynamic parameters are not always concurrently driven by ABP.

B. Average Baseline Phasor Ratios

Fig. 4 shows the average phasor ratios at 0.1 Hz over channels and sessions for each subject (Fig. 4(a), (b), and (c)), and over subjects and sessions for each channel (Fig. 4(d), (e), and (f)).

TABLE I
AVERAGE AMPLITUDE RATIO AND PHASE DIFFERENCE FOR EACH BLOCK

BL	|O/ABP| (μM/mmHg)	∠O/ABP (Deg.)	|D/ABP| (μM/mmHg)	∠D/ABP (Deg.)	|D/O| (-)	∠D/O (Deg.)
1	0.10 ± 0.06	-30 ± 30	0.02 ± 0.03	110 ± 60	0.2 ± 0.6	150 ± 70
2	0.10 ± 0.06	-40 ± 30	0.02 ± 0.03	100 ± 70	0.2 ± 0.2	140 ± 70
3	0.10 ± 0.06	-40 ± 30	0.02 ± 0.03	110 ± 70	0.2 ± 0.3	140 ± 70
4	0.10 ± 0.06	-40 ± 30	0.02 ± 0.03	100 ± 70	0.2 ± 0.3	140 ± 70
5	0.10 ± 0.06	-40 ± 30	0.02 ± 0.04	110 ± 70	0.2 ± 0.4	150 ± 70
6	0.10 ±0.06	-40 ± 30	0.02 ± 0.03	100 ± 70	0.2 ± 0.3	140 ± 70

O = Oxy hemoglobin phasor, D = Deoxy hemoglobin phasor, ABP = Arterial Blood Pressure phasor, BL = Block

Averaging over the channels and sessions gives insight into the variability across subjects. The lowest spread in phase was seen in **O/ABP** (Fig. 4(a)), while **D/ABP** varied by ∼120 degrees, with varying amplitude ratios across subjects. For **D/ABP** and **D/O**, as the phase difference approached 0 the amplitude decreased. Averaging over subjects and sessions for each channel gives insight onto the spatial variability over the probed brain region. Neither **O/ABP**, **D/ABP** or **D/O** (Fig. 4(d), (e), and (f)) show significant differences among the channels.

The average over channels, subjects, and session for **O/ABP**, **D/ABP**, and **D/O** is shown in Fig. 5(a), (b), and (c), allowing for an examination of the range amongst the population. The phase standard deviation was ∼30 degrees for **O/ABP**, ∼60 degrees for **D/ABP**, and ∼70 degrees for **D/O**. For the amplitude ratio, **|D/ABP|** had the lowest standard deviation of 0.03 μM/mmHg, while it was 0.06 μM/mmHg for **|O/ABP|**.

C. Average Phasor Ratios Between Blocks

Fig. 6 reports the average phasor ratios across all subjects, sessions, and channels for the 6 blocks. Braking events occurred randomly for every subject/session, and due to their approximate timing during the experiment it was assumed that at least one event occurred during each block. The average phasor ratios for **O/ABP**, **D/ABP**, and **D/O** for each block (denoted by a different color) is shown in Fig. 6. All phasor ratios lie within the standard deviations and are overlapping, which shows no difference between all 6 blocks. Table I reports the average amplitude ratio and phase difference with the standard deviation for each block, where block 1 is the baseline. **O/ABP** showed the smallest deviation between the blocks and overall variability.

IV. DISCUSSION

An in-depth analysis was performed to evaluate the amount of time with coherent hemodynamics at frequencies between 0.01 and 1.5 Hz. The heart rate showed the highest amount, which has previously been reported [6], and is expected due to arterial pulsation contributions to ΔO measurements. The lower fraction of time from ΔD can be explained by the small ΔD signal (and

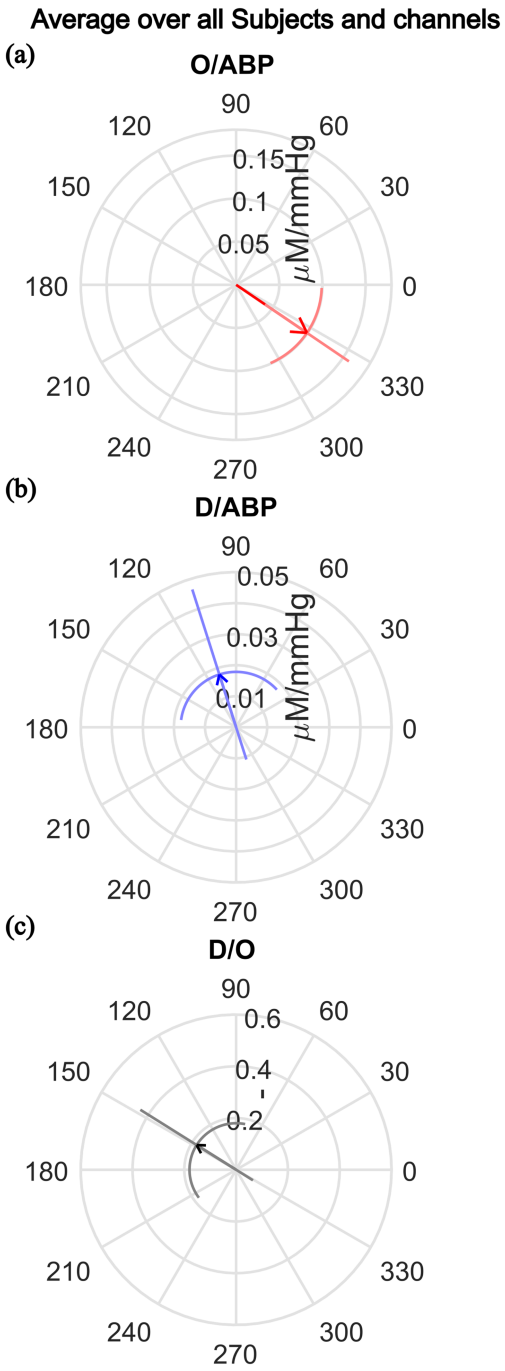

Fig. 5. Average phasor ratio across subject, channel, and session at baseline for (a) oxy (**O**) hemoglobin versus arterial blood pressure (**ABP**), (b) deoxy (**D**) hemoglobin versus **ABP**, (c) **D** versus **O**.

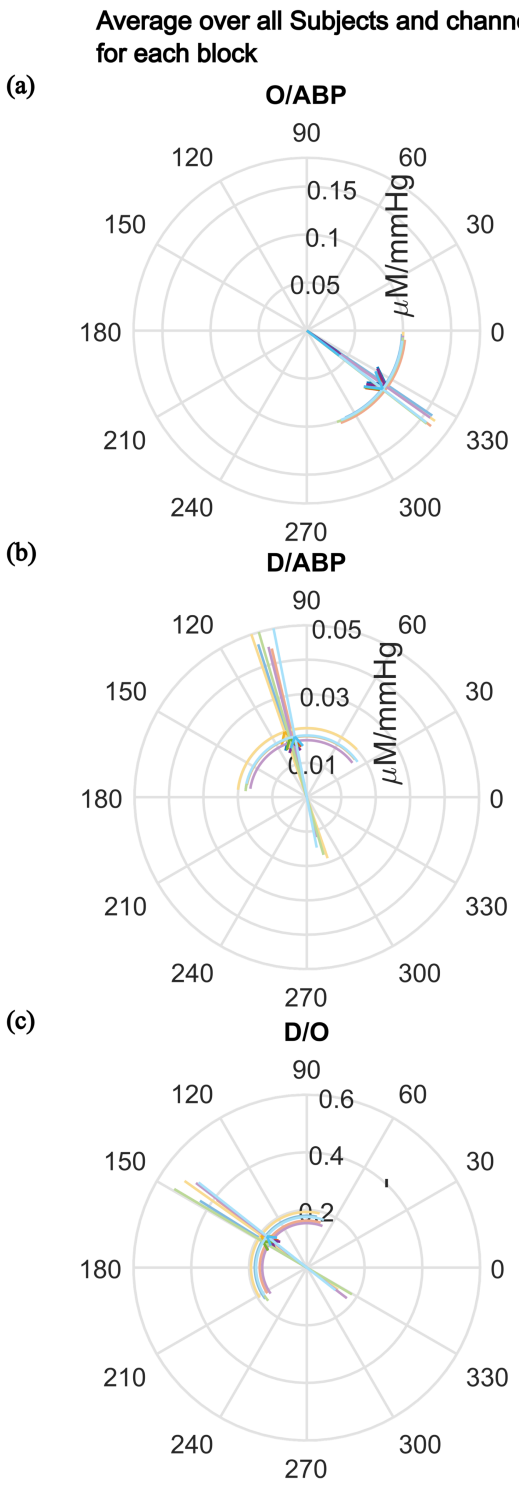

Fig. 6. Average phasor ratio for (a) oxy (**O**) hemoglobin versus arterial blood pressure (**ABP**), (b) deoxy (**D**) hemoglobin versus ABP, and (c) **D** versus **O** for each of the 6 blocks (shown as one individual color).

thus small signal-to-noise) originating from the arteries due to high oxygen saturation of arterial blood.

For LFOs, ∼0.1 Hz showed the highest fraction of time with coherence for **O/ABP**, **D/ABP**, and the logical AND between **O/ABP** and **D/ABP** (Fig. 3(a)). A peak at ∼0.1 Hz has previously been shown [6], [12]. This frequency is associated with Mayer waves, which are linked with spontaneous oscillations in ABP and oscillations in sympathetic nerve activity [8]. These systemic oscillations drive cerebral hemodynamics and account for the high coherence observed. Previous studies considered a low number of subjects (3 and 13, respectively [6], [12]), while the results presented in Fig. 3 allows for examination of variability across the 78 subjects, 2 sessions and 20 channels. This study shows the promise of using spontaneous oscillations for Coherent Hemodynamics Spectroscopy (CHS) given that in

3-minutes, on average, ∼30% of time features coherent cerebral hemodynamics at 0.1 Hz in as many as half of the NIRS channels used in this study.

Spontaneous and induced oscillations at 0.1 Hz have been used in combination with NIRS [6], [11], [16] to study the relationship between hemodynamics and ABP. In this study, **D/O** had an average amplitude ratio (∼0.18) and phase difference (∼−212 degrees) that aligns with reported results on 5 subjects with repeated induced oscillation measurements at 0.1 Hz and 30 mm source-detector separation [24]. The mean phase difference for all phasor ratios aligned with reported results on healthy human subjects [10], [25].

The phase difference between **O** and **ABP** had the lowest standard deviation in all blocks (Table I). Higher variability in **D/ABP** and **D/O** can be explained by their sensitivity to changes in blood flow, a higher sensitivity to blood volume changes in superficial tissue, and a lower signal-to-noise associated with measurements of ΔD. Assuming a constant **O/ABP** a relative increase in blood volume contributions versus blood flow contributions to the optical measurements would shift **D/ABP** towards **O/ABP** and cause a decrease in its amplitude [20]. This was seen for **D/ABP** over subjects (Fig. 4(b)) and could explain the larger variability as the contribution of blood volume to the optical signal differed for each subject.

Spatial averages (Fig. 4(d), (e), and (f)) showed no qualitative significant differences between channels suggesting spatially uniform cerebral hemodynamics associated with systemic changes in ABP [26], [27]. Variability among the subjects (Fig. 4(a), (b), and (c)) was larger than across the channels and indicates that subjects may be separable from each other resulting from individual cerebrovascular or anatomical features.

Comparison between baseline and other blocks that involved a braking task showed no qualitative significant difference (Fig. 6). This implies that there were no detectable changes in the relative dynamics of cerebral hemodynamics and ABP during the driving events. Previous work showed an increase in the wavelet coefficient amplitude between straight driving and driving mixed with tasks in the frequency range of 0.0095–0.021 Hz on the pre-frontal cortex [28] but not at the frequency band including 0.1 Hz for ΔO which aligns with presented results.

V. Conclusion

Cerebral hemodynamics coherent with systemic ABP provide indications on the health of cerebral perfusion and autoregulation [10], [19], [29]. Measurements of cerebral hemodynamics (specifically, O and D) with NIRS are non-invasive and reflect blood volume, blood flow, and rate of oxygen delivery to tissue at the microcirculation level [9], [10]. This work has shown that NIRS can measure spontaneous cerebral hemodynamic oscillations in the autoregulation frequency range of 0.1 Hz that show a significant coherence and meet strict requirements with ABP for about 10%-30% of the measurement time. This result means that spontaneous coherent hemodynamics can be measured with NIRS to evaluate cerebral perfusion health and efficiency of cerebral autoregulation, at least when measurements can be performed over a time of at least a few minutes and physiological conditions remain stable during this period. Another implication of this work is that CHS [30], [31] may be based on spontaneous rather than induced ABP and cerebral hemodynamic oscillations, provided that proper care is taken in identifying significant levels of coherence which is needed to ensure changes in ABP are the driving forces for the hemodynamic changes. The possibility of relying on spontaneous hemodynamics rather than induced hemodynamics has important practical implications as subjects would not be required to undergo physiological maneuvers or perturbations. Finally, the finding of a lack of significant effects of braking tasks on the relative amplitude and phase of coherent cerebral hemodynamics and ABP may be specific to this measurement protocol. Future work will involve functional brain activation with a variety of motor, visual, or cognitive workloads for a more thorough characterization of coherent cerebral hemodynamics during brain activation.

References

[1] D. Phillip, H. Schytz, H. Iversen, J. Selb, D. Boas, and M. Ashina, "Spontaneous low frequency oscillations in acute ischemic stroke – A near infrared spectroscopy (NIRS) study," *J. Neurol. Neurophysiol.*, vol. 5, no. 6, pp. 1–5, Oct. 2014, doi: 10.4172/2155-9562.1000241.

[2] D. A. Boas, A. M. Dale, and M. A. Franceschini, "Diffuse optical imaging of brain activation: Approaches to optimizing image sensitivity, resolution, and accuracy," *Neuroimage*, vol. 23, no. Suppl 1, pp. S275–S288, 2004, doi: 10.1016/j.neuroimage.2004.07.011.

[3] K.-S. Hong and M. A. Yaqub, "Application of functional near-infrared spectroscopy in the healthcare industry: A review," *J. Innov. Opt. Health Sci.*, vol. 12, no. 06, Nov. 2019, Art. no. 1930012, doi: 10.1142/S179354581930012X.

[4] J. E. Mayhew et al., "Cerebral vasomotion: A 0.1-hz oscillation in reflected light imaging of neural activity," *Neuroimage*, vol. 4, no. 3 Pt 1, pp. 183–193, Dec. 1996, doi: 10.1006/nimg.1996.0069.

[5] T. J. Huppert, R. D. Hoge, S. G. Diamond, M. A. Franceschini, and D. A. Boas, "A temporal comparison of BOLD, ASL, and NIRS hemodynamic responses to motor stimuli in adult humans," *Neuroimage*, vol. 29, no. 2, pp. 368–382, Jan. 2006, doi: 10.1016/j.neuroimage.2005.08.065.

[6] H. Obrig et al., "Spontaneous low frequency oscillations of cerebral hemodynamics and metabolism in human adults," *NeuroImage*, vol. 12, no. 6, pp. 623–639, Dec. 2000, doi: 10.1006/nimg.2000.0657.

[7] I. Tachtsidis, M. Tisdall, D. T. Delpy, M. Smith, and C. E. Elwell, "Measurement of cerebral tissue oxygenation in young healthy volunteers during acetazolamide provocation: A transcranial doppler and near-infrared spectroscopy investigation," in *Oxygen Transport to Tissue XXIX*. Boston, MA, USA: Springer, 2008, pp. 389–396, doi: 10.1007/978-0-387-74911-2_43.

[8] A. Sassaroli, M. Pierro, P. R. Bergethon, and S. Fantini, "Low-frequency spontaneous oscillations of cerebral hemodynamics investigated with near-infrared spectroscopy: A review," *IEEE J. Sel. Topics Quantum Electron.*, vol. 18, no. 4, pp. 1478–1492, Jul./Aug. 2012, doi: 10.1109/JSTQE.2012.2183581.

[9] M. W.-D. Müller, M. Österreich, A. Müller, and J. Lygeros, "Assessment of the Brain's macro- and micro-circulatory blood flow responses to CO2 via transfer function analysis," *Front Physiol.*, vol. 7, May 2016, Art. no. 162, doi: 10.3389/fphys.2016.00162.

[10] M. Reinhard et al., "Oscillatory cerebral hemodynamics—The macro- vs. microvascular level," *J. Neurological Sci.*, vol. 250, no. 1, pp. 103–109, Dec. 2006, doi: 10.1016/j.jns.2006.07.011.

[11] C. E. Elwell, R. Springett, E. Hillman, and D. T. Delpy, "Oscillations in cerebral haemodynamics. Implications for functional activation studies," *Adv. Exp. Med. Biol.*, vol. 471, pp. 57–65, 1999.

[12] E. Kirilina, N. Yu, A. Jelzow, H. Wabnitz, A. Jacobs, and I. Tachtsidis, "Identifying and quantifying main components of physiological noise in functional near infrared spectroscopy on the prefrontal cortex," *Front. Hum. Neurosci.*, vol. 7, 2013, Art. no. 864, doi: 10.3389/fnhum.2013.00864.

[13] A. Sassaroli, X. Zang, K. T. Tgavalekos, and S. Fantini, "Induced and spontaneous hemodynamic oscillations in cerebral and extracerebral tissue for coherent hemodynamics spectroscopy," *Proc. SPIE*, vol. 10059, pp. 138–145, Feb. 2017, doi: 10.1117/12.2250930.

[14] T. McWilliams, N. Ward, B. Mehler, and B. Reimer, "Assessing driving simulator validity: A comparison of multi-modal smartphone interactions across simulated and field environments," *Transp. Res. Rec.*, vol. 2672, no. 37, pp. 164–171, Dec. 2018, doi: 10.1177/0361198118798729.

[15] C. Jeleazcov et al., "Precision and accuracy of a new device (CNAP^{TM}) for continuous non-invasive arterial pressure monitoring: Assessment during general anaesthesia," *Brit. J. Anaesth.*, vol. 105, no. 3, pp. 264–272, Sep. 2010, doi: 10.1093/bja/aeq143.

[16] G. Blaney, A. Sassaroli, T. Pham, C. Fernandez, and S. Fantini, "Phase dual-slopes in frequency-domain near-infrared spectroscopy for enhanced sensitivity to brain tissue: First applications to human subjects," *J. Biophotonics*, vol. 13, no. 1, 2020, Art. no. e201960018, doi: 10.1002/jbio.201960018.

[17] B. Hallacoglu, A. Sassaroli, and S. Fantini, "Optical characterization of two-layered turbid media for non-invasive, absolute oximetry in cerebral and extracerebral tissue," *PLoS One*, vol. 8, no. 5, May 2013, Art. no. e64095, doi: 10.1371/journal.pone.0064095.

[18] G. Blaney, C. Fernandez, A. Sassaroli, and S. Fantini, "Dual-slope imaging of cerebral hemodynamics with frequency-domain near-infrared spectroscopy," *NPh*, vol. 10, no. 1, Jan. 2023, Art. no. 013508, doi: 10.1117/1.NPh.10.1.013508.

[19] T. Pham et al., "Noninvasive optical measurements of dynamic cerebral autoregulation by inducing oscillatory cerebral hemodynamics," *Front. Neurol.*, vol. 12, 2021, Art. no. 745987, doi: 10.3389/fneur.2021.745987.

[20] K. Khaksari, G. Blaney, A. Sassaroli, N. Krishnamurthy, T. Pham, and S. Fantini, "Depth dependence of coherent hemodynamics in the human head," *J. Biomed. Opt.*, vol. 23, no. 12, Nov. 2018, Art. no. 121615, doi: 10.1117/1.JBO.23.12.121615.

[21] G. Blaney, A. Sassaroli, and S. Fantini, "Algorithm for determination of thresholds of significant coherence in time-frequency analysis," *Biomed. Signal Process. Control*, vol. 56, Feb. 2020, Art. no. 101704, doi: 10.1016/j.bspc.2019.101704.

[22] A. Sassaroli, K. Tgavalekos, and S. Fantini, "The meaning of 'coherent' and its quantification in coherent hemodynamics spectroscopy," *J. Innov. Opt. Health Sci.*, vol. 11, no. 6, Nov. 2018, Art. no. 1850036, doi: 10.1142/S1793545818500360.

[23] A. V. Andersen, S. A. Simonsen, H. W. Schytz, and H. K. Iversen, "Assessing low-frequency oscillations in cerebrovascular diseases and related conditions with near-infrared spectroscopy: A plausible method for evaluating cerebral autoregulation?," *Neurophotonics*, vol. 5, no. 3, Sep. 2018, Art. no. 030901, doi: 10.1117/1.NPh.5.3.030901.

[24] G. Blaney, A. Sassaroli, T. Pham, N. Krishnamurthy, and S. Fantini, "Multi-distance frequency-domain optical measurements of coherent cerebral hemodynamics," *Photonics*, vol. 6, no. 3, Sep. 2019, Art. no. 3, doi: 10.3390/photonics6030083.

[25] G. Blaney, A. Sassaroli, and S. Fantini, "Dual-slope imaging in highly scattering media with frequency-domain near-infrared spectroscopy," *Opt. Lett.*, vol. 45, no. 16, Aug. 2020, Art. no. 4464, doi: 10.1364/OL.394829.

[26] T. Katura, N. Tanaka, A. Obata, H. Sato, and A. Maki, "Quantitative evaluation of interrelations between spontaneous low-frequency oscillations in cerebral hemodynamics and systemic cardiovascular dynamics," *NeuroImage*, vol. 31, no. 4, pp. 1592–1600, Jul. 2006, doi: 10.1016/j.neuroimage.2006.02.010.

[27] M. L. Pierro, A. Sassaroli, P. R. Bergethon, B. L. Ehrenberg, and S. Fantini, "Phase-amplitude investigation of spontaneous low-frequency oscillations of cerebral hemodynamics with near-infrared spectroscopy: A sleep study in human subjects," *NeuroImage*, vol. 63, no. 3, pp. 1571–1584, Nov. 2012, doi: 10.1016/j.neuroimage.2012.07.015.

[28] G. Xu et al., "Functional connectivity analysis of distracted drivers based on the wavelet phase coherence of functional near-infrared spectroscopy signals," *PLoS One*, vol. 12, no. 11, Nov. 2017, Art. no. e0188329, doi: 10.1371/journal.pone.0188329.

[29] C. Zweifel et al., "Continuous assessment of cerebral autoregulation with near-infrared spectroscopy in adults after subarachnoid hemorrhage," *Stroke*, vol. 41, no. 9, pp. 1963–1968, Sep. 2010, doi: 10.1161/STROKEAHA.109.577320.

[30] J. M. Kainerstorfer, A. Sassaroli, K. T. Tgavalekos, and S. Fantini, "Cerebral autoregulation in the microvasculature measured with near-infrared spectroscopy," *J. Cereb. Blood Flow Metab.*, vol. 35, no. 6, pp. 959–966, Jun. 2015, doi: 10.1038/jcbfm.2015.5.

[31] S. Fantini, "Dynamic model for the tissue concentration and oxygen saturation of hemoglobin in relation to blood volume, flow velocity, and oxygen consumption: Implications for functional neuroimaging and coherent hemodynamics spectroscopy (CHS)," *NeuroImage*, vol. 85, pp. 202–221, Jan. 2014, doi: 10.1016/j.neuroimage.2013.03.065.